ELSEVIER

Nuclear Instruments and Methods in Physics Research A 446 (2000) 222–228

NUCLEAR INSTRUMENTS & METHODS IN PHYSICS RESEARCH Section A

www.elsevier.nl/locate/nima

The HERA-B vertex detector: first results from detector commissioning

Wolfgang Wagner*

For the HERA-B Collaboration

Max-Planck-Institut für Physik, Föhringer Ring 6, 80805 München, Germany

Abstract

An overview of the design of the HERA-B vertex detector is presented. During the 1998/99 commissioning run 25% of the system was instrumented. First results from this data taking period are shown.

1. The basic design

The vertex detector of the HERA-B experiment [1,2] has to provide the data for precise reconstruction of the primary vertices at the target and the secondary decay vertices of particles with lifetimes $\tau > 10^{-12}$ s. The data of the vertex detector contribute to the second level trigger of the experiment. The system covers an acceptance from 10 up to 250 mrad vertically and horizontally. We require an impact parameter resolution of $\sigma \approx 25\ \mu\text{m} \oplus 30\ \mu\text{m}/p_t$ (GeV). The vertex resolution must be $\sigma_z \approx 500\ \mu$m longitudinal and $\sigma_{xy} \approx 25\ \mu$m transverse to the beam. The longitudinal vertex resolution should be compared to the mean decay length of B-mesons in HERA-B which is 11.8 mm.

The vertex detector has a larger acceptance then the main tracking system in order to achieve the best possible efficiency for vertexing. Therefore, an efficient and fast tracking procedure for independent pattern recognition and tracking is needed.

The vertex detector is based on double-sided silicon strip detectors which are mounted in planes perpendicular to the beam. The detectors are arranged in eight superlayers and four quadrants. Each quadrant of a superlayer contains two silicon microstrip detectors. In total this amounts to 64 detectors. The double-sided option was chosen in order to minimize the material.

Each detector has an active area of $50 \times 70\ \text{mm}^2$. The strips are tilted by 2.5° with respect to the edge of the detector. This allows a stereo angle of 5.0° when mounting two detectors back to back. The pitch of the implanted strips is 27.33 μm on the n-side and 25.88 μm on the p-side. Every second strip is metallized and read out, resulting in a readout pitch of 54.67 μm on the n-side and 51.75 μm on the p-side. The charge collected at the intermediate strips, which are not read out, is spread via capacitive coupling to the neighboring

* Tel.: +49-89-32354-240; fax: +49-89-3226704.
E-mail address: wagner@mppmu.mpg.de (W. Wagner).

0168-9002/00/$ - see front matter
PII: S0168-9002(00)00024-3

readout strips. The narrow readout pitch is chosen not only to provide good intrinsic resolution, but primarily to limit the occupancy of the detector strips to a maximum of 5%. More details on the detector design and the technology can be found in Refs. [3–5].

A single-silicon wafer has 1280 readout strips on the n-side and 1024 on the p-side. In total the vertex system comprises 147,000 channels with analog readout, allowing optimal position resolution and control of common mode fluctuations.

Due to the high interaction rate of 40 MHz the silicon detectors experience severe radiation damage, which results in an increase of the leakage current and an increase of the depletion voltage. The detectors must be capable to hold bias voltages up to 500 V. In the area close to the beam a maximum radiation dose of 100 kGy per year is expected. The particle flux drops like $1/R_{\perp}^2$, where $R_{\perp}$ is the radial distance to the beam center. Thus, the radiation damage is highly inhomogeneous. However, to keep the entire detector operational the maximum dose at the hot spot is relevant. The detectors are designed to survive one HERA-B year of running at the design interaction rate of 40 MHz. It is foreseen to exchange the silicon detectors once per year.

At the MPI für Kernphysik in Heidelberg a single-sided detector was inhomogeneously irradiated with protons of a kinetic energy of $E_{\mathrm{kin}} = 20$ MeV in order to investigate the performance of the detectors after irradiation [6,7]. The peak fluence was equivalent to 2.7×10^{14} cm^{-2} minimum ionizing particles (MIPs), i.e. similar to the radiation dose of one HERA-B year at the design interaction rate of 40 MHz. The most irradiated strips show a signal-to-noise ratio of $S/N = 14$ (peak position). Before irradiation the value was $S/N = 21$. This result suggests that the detectors can be operated at a tolerable noise level after one HERA-B year.

2. The technology

During data taking the silicon detectors must be placed at a distance of 10 mm from the beam. On the other hand the detectors must be retracted from the beam during the injection of the protons into the HERA ring. To fulfill both requirements HERA-B decided to employ a Roman pot system with movable pots. The Roman pots are mounted on manipulators allowing radial and lateral movements. By moving the pots laterally to the beam the detectors can be placed in two different configurations around the beam. By changing the position regularly, about once per month, the radiation dose at the hot spots near the beam is reduced. The lifetime of the detectors is increased by roughly a factor of two.

Ideally, one would want to operate the detectors directly in the vacuum of the HERA storage ring. However, since the ultra-high vacuum conditions required by the machine cannot be guaranteed by the detector environment with its components and vacuum feed-throughs, the VDS modules are operated in a secondary vacuum which is separated from the primary vacuum of the machine by 150 μm thin aluminum caps. These caps have the additional benefit that they also shield the electronics from wake fields of the beam.

The Roman pots are placed in a 2.20 m long stainless-steel vessel which is schematically depicted in Fig. 1. The HERA proton beam passes through the center of the vessel which has to be kept at a primary vacuum of 10^{-8} mbar. The secondary vacuum inside the caps is 10^{-6} mbar.

Since the vacuum vessel also acts as an RF-cavity with respect to the beam, four 5 μm thin stainless-steel bands are installed to form a RF-shield reducing wake fields inside the vessel [8]. These steel bands are 13 mm wide and surround the beam at a distance of 7 mm. During injection they are retracted together with the Roman pots.

While the vacuum vessel houses seven superlayers of the silicon detector, the eighth superlayer is placed outside, behind the exit flange of the vessel.

The silicon detectors and the readout electronics are mounted on carbon fiber plates and form a so-called detector module which is schematically shown in Fig. 2. The silicon detectors are glued to the carbon fiber carrier using a silicone adhesive which remains elastic after solidifying [10]. Thereby mechanical stress resulting in a high leakage current is prevented.

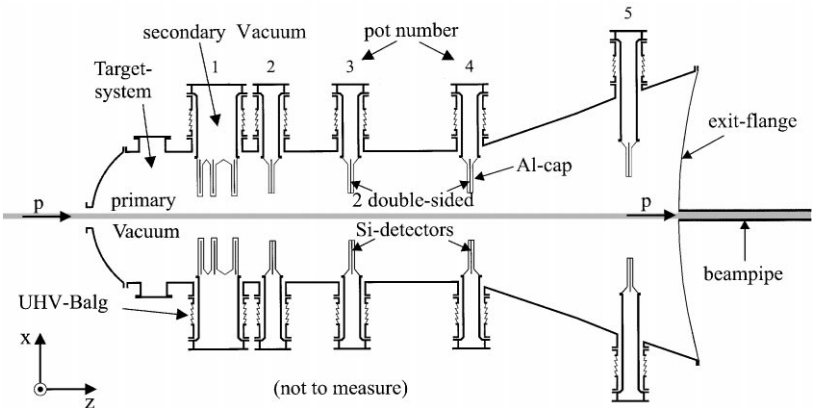

Fig. 1. The vertex vessel. The drawing shows a vertical cut through the vertex vessel which houses 20 Roman pots. These pots are arranged in five layers and four quadrants. The pots of the first layer contain six silicon detectors, while the pots of the other layers contain two silicon detectors. In total there are 56 silicon detectors mounted inside the vacuum vessel. During operation the detectors inside the first four pots are positioned such that the innermost edge of the active area is located at a radial distance of 10 mm from the beam. The detectors in pot five have a distance of 12 mm from the beam.

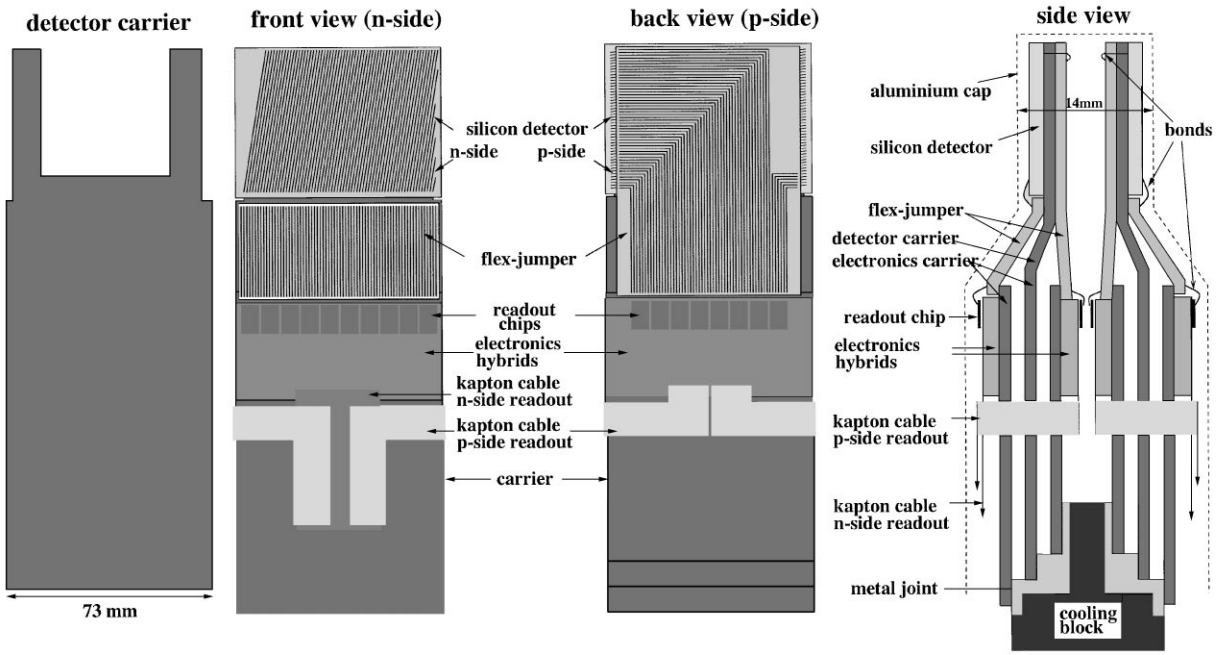

Fig. 2. Schematic view of a detector module. On the left of the picture the carbon carrier is depicted. At the front end the carrier is fork-shaped in order to minimize the material in the acceptance. In the center of the picture the front and the back view of the detector module are shown. The detector strips are tilted by 2.5° with respect to the detector edge, while the strips on the front side and on the back side have an angle of 90.0° with respect to each other. The readout chips are placed on an electronics hybrid. On the right-hand side of the figure a side view of two detector modules is shown. The scale is distorted. The two modules are mounted back to back and attached to a common cooling block. In order to thermally decouple the electronics and the detector, the hybrids and the silicon wafer are placed on separate carbon fiber plates.

The detector modules are equipped with HELIX128 readout chips [9] which were developed at the University of Heidelberg. They are radiation resistant up to dose of 2 kGy [9]. The readout chips are placed at a distance of 10 cm from the beam, thereby lowering the radiation dose by a factor of 100 compared to the innermost detector edge.

The detector strips and the readout channels on the HELIX-chips are connected by a flexible pitch adaptor. This flex-jumper consists of two kapton foils with copper traces on both sides. By gluing two kapton foils on top of each other using an appropriate offset the pitch of the detector strips is achieved. On the p-side the copper traces reach a length of up to 16 cm. These long traces result in high load capacitances on the p-side, thereby generating additional noise in the electronics. The detector strips, the copper traces on the flex-jumper and the pads on the HELIX-chips are connected by ultra sonic wedge-bonding.

Two modules are mounted back to back and form one quadrant of a superlayer providing four views of a particle track: $+2.5^\circ$, $+92.5^\circ$, $+87.5^\circ$ and $+177.5^\circ$. The layout of the VDS is such that a track from the primary vertex traverses at least three superlayers. With four views per superlayer the VDS provides redundancy for high-efficiency standalone tracking. For the first data taking periods the first three superlayers, for technical reasons, will be instrumented with one double-sided and one single-sided detector, thus providing three views. This reduces the redundancy, but still allows independent tracking.

3. The setup during the 1998/99 run

For commissioning of the vertex detector about 25% of the system was installed in May 1998. There were 14 double-sided and 3 single-sided detector modules mounted in the superlayers 3, 4, 5 and 6. Except for superlayer 6 the modules were only placed in the lower and outer quadrants covering an L-shaped geometrical acceptance. These modules were equipped with HELIX128-2.1 readout chips.

In December 1998 the two modules in the outer quadrant of superlayer 5 were replaced with new modules carrying the HELIX128-2.2 readout chips and improved electronics hybrids. Additionally, one detector module was installed in superlayer 8 outside of the vertex vessel.

The vertex detector was integrated into the common data acquisition and the slow control of HERA-B. Software tools for online monitoring were set up. The online histograms show the signal-to-noise ratios and the occupancies of all detector sides. The package contains also a simple event display which illustrates the raw data processing and the hit selection.

Moving the Roman pots to their data taking position has become a standard procedure within HERA-B. Software for alignment of the detectors using tracks was established. The analysis of the data taken in 1998/99 is still ongoing.

In May 1999 the VDS was instrumented with 44 out of 64 detectors. Six of these detectors are single-sided and they are placed in the first three superlayers. The rest of the system will be installed in December, thus completing the VDS.

4. Signal-to-noise ratio and cluster sizes

The signal-to-noise ratios of the detectors and the cluster sizes were investigated in a first analysis of the data from the commissioning run. The results are shown in Fig. 3. The data were taken from a module equipped with the HELIX128-2.2 chip.

In the signal-to-noise (S/N) distributions the peak of minimum-ionizing particles (MIPs) is clearly separated from the noise peak. On the n-side the MIP-peak is well above 20, while on the p-side the distribution peaks around 17. This reduction is due to the higher load capacitances on the p-side. Single-plane efficiencies above 99% are reached with these modules. For the previous version of the HELIX chip, HELIX128-2.1, the signal-to-noise ratio is somewhat lower, between 12 and 16.

Table 1 gives an overview of the cluster sizes. The values shown were obtained using a cut of $S/N = 3$ for each single-detector strip and a cut of $S/N = 5$ for the entire cluster. More than half of the clusters have a width of two strips. These clusters originate from particles traversing the silicon detectors in the

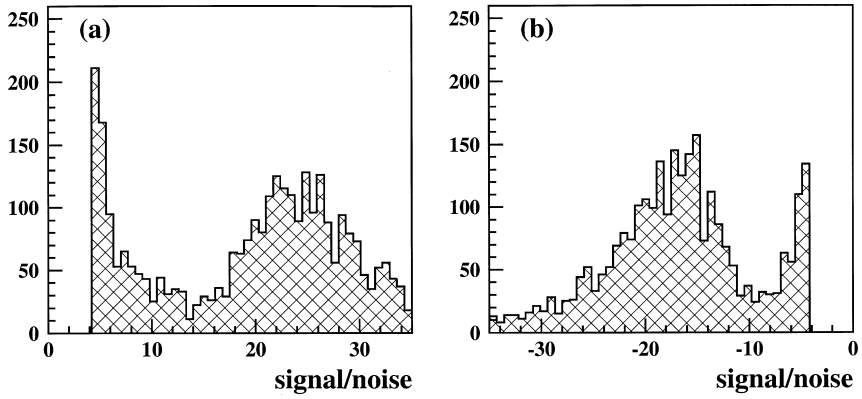

Fig. 3. Typical signal-to-noise ratios. (a) shows the signal-to-noise ratio on the n-side of the detector; (b) the signal-to-noise ratio on the p-side. The data were taken with a module which was equipped with the final electronics: the HELIX128-2.2 chip. A cut of $S/N \geqslant 4$ is applied by the cluster finding algorithm.

Table 1
Distribution of the cluster widths

Cluster size (strips)	Percentage
1	25
2	54
3	16
4	3
$\geqslant 5$	2

Note: The given values were obtained using a cut of $S/N = 3$ for each single-detector strip and a cut of $S/N = 5$ for the entire cluster.

area between two readout strips. In one quarter of the cases the clusters consist only of one strip. These clusters are due to particles passing through the implanted area of the readout strips. The measured cluster width distributions agree with those expected from laser measurements performed on a teststand in the laboratory [11,12].

Clusters with two or more strips allow the exploitation of the analog readout. Calculating the center of charge of the cluster gives a much better estimate of the impact point of the particle than taking the simple digital information. To improve the detector resolution without increasing the number of readout channels we have chosen to place one intermediate strip between two readout strips. This results in a higher percentage of two-strip clusters, thereby increasing the resolution.

5. Reconstruction of the target spot

The tracks found in the vertex detector are used to reconstruct the interaction region at the target. The tracks are extrapolated into the x–y plane at the z-position of the target. The intersection point of the target plane and the track is histogrammed. The peak position of the resulting distribution is shown in Fig. 4 as a function of time. In the plot the target position as measured by the mechanical target steering is overlayed. The two curves agree very well within the errors. The plot illustrates how the target was constantly moved in order to keep the interaction rate stable. Within one and a half hour the target moved towards beam by about 60 μm. The presented results indicate that the vertex detector will be a valuable tool for target diagnostics, especially if the interaction rate has to be equally distributed over several wires running in parallel.

Using the tracks originating from the target the vertex detector modules are aligned with respect to each other. The starting point for this procedure is provided by a survey during the installation. The current stage of alignment results in track residuals below 30 μm.

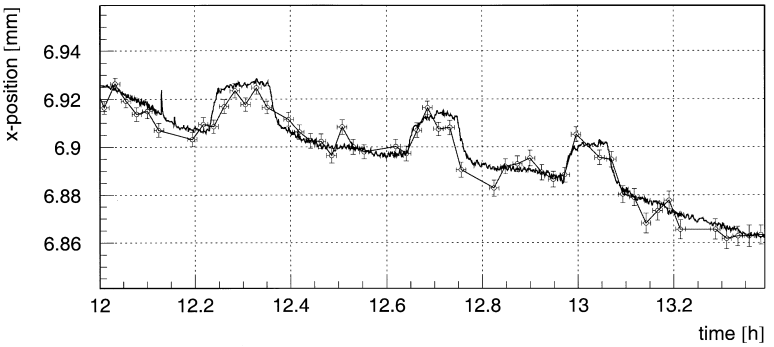

Fig. 4. Overlay of the reconstructed target spot (crosses) and the target position (line) as measured by the mechanical target steering.

Table 2
Results of a tracking efficiency study using events generated in a Monte Carlo simulation

Det. Effic. (%)	Ref. Tracks (%)	Clones (%)	Ghosts (%)	Time (ms)
100	95.0	3.8	15.2	215
95	94.6	3.5	15.3	190
90	93.2	3.3	16.3	169

Note: The detector noise was not included in this simulation.

6. Tracking performance

Two software packages for independent pattern recognition and track reconstruction have been developed. The first package, HOLMES [13], is based on a Kalman filter algorithm, the second one, CATS [14], on a cellular automaton [15]. The performance of the tracking codes was determined from Monte Carlo simulations. Both programs show compatible results [16].

Table 2 provides the reconstruction probability for reference tracks, the clone rate, the ghost rate and the time needed for reconstruction for three different detector efficiencies. Reference tracks are defined as those passing through three superlayers and having a momentum of $p > 1$ GeV. The reconstruction probability for these tracks stays above 93% for all assumed detector efficiencies. The clone rate is below 4%. The ghost rate only depends weakly on the detector efficiency and is stable at about 15%. The reconstruction time is around 200 ms, which is fast enough compared to the reconstruction of an entire HERA-B event which should be finished within 4 s [17].

Fig. 5 shows the reconstruction probability as a function of the event multiplicity and the inverse track momentum. The mean event multiplicity in this study was 4, Poisson distributed. The reconstruction probability for reference tracks drops from 99% for one event to about 85% for nine superimposed events, while the ghost rate rises from 5% to 15%. The clone rate is below 5% over the whole range of the event multiplicity. A clone track is due to a particle which experiences hard scattering inside the silicon detector, such that its track is reconstructed as two separate tracks. One of these tracks is counted as real and the other one as a clone. The clone rate, as seen by the reconstruction programs, is at the expected level.

The reconstruction probability for high momentum tracks is 97% and decreases for tracks of 1 GeV/c to 92%. The first number is the one relevant for particles originating from B-decays. The clone rate for low momentum tracks is about 7%. As multiple scattering decreases with increasing momentum the clone rate goes down to less than 1%.

7. Conclusions

- More than two thirds of the vertex detector system of the HERA-B experiment was installed in

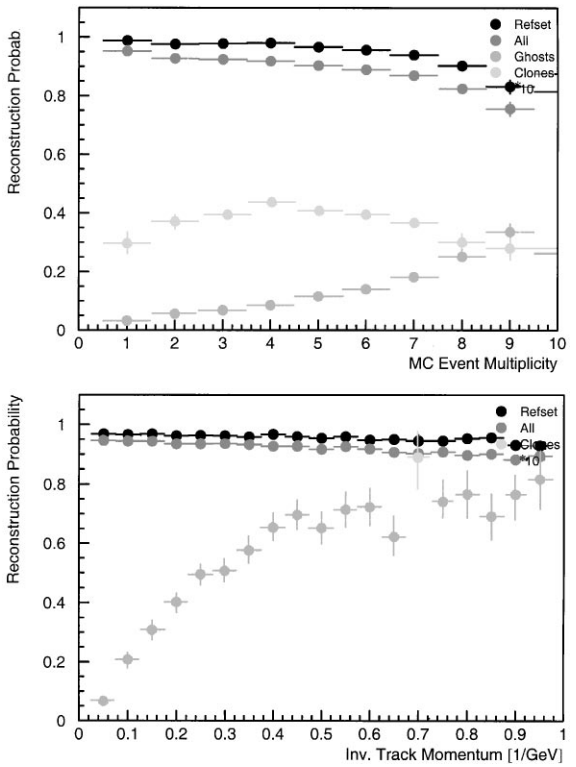

Fig. 5. Reconstruction probability versus event multiplicity and inverse track momentum. The curves show results of a Monte Carlo study using 1000 simulated events with a mean of four superimposed interactions per event (Poisson distributed). The results of these plots were obtained assuming a detector efficiency of 100%. No noise was added in this simulation. The numbers for clones are multiplied by 10 in the histograms. Ghosts do not appear in the momentum plot, since they have no momentum. The reference tracks (Refset) are the relevant sample of tracks. They hit three superlayers of the VDS and have a momentum above 1 GeV. The set of tracks labeled "All" contains also tracks which hit only two superlayers. No momentum cut is applied. These tracks are used in order to study the performance of the codes in case of relaxed track requirements.

May 1999. The rest of the system will be completed by the end of the year.

- The commissioning of the vertex detector system is underway.
- The final detector modules achieve a signal-to-noise ratio of $S/N \simeq 20$. Those modules achieve a single-plane efficiency above 99%.
- Two reconstruction programs are available. The reconstruction probability is about 95% and the ghost rate is about 15%. Further studies are ongoing, including work on detector data.

Acknowledgements

I would like to thank my colleagues Dr. Iris Abt, Martin Bräuer, Dr. Thorsten Glebe, Dr. Ivan Kisel, and Thomas Perschke who helped me to collect the information and the plots for this talk.

References

[1] T. Lohse et al. (HERA-B Collaboration), An experiment to study CP violation in the B system using an internal target at the HERA proton ring, HERA-B Proposal, DESY-PRC 94/02, 1994.
[2] E. Hartouni et al., (HERA-B Collaboration), HERA-B Technical Design Report, DESY-PRC 95/01, 1995.
[3] A. Bischoff et al., Nucl. Instr. and Meth. A 326 (1993) 27.
[4] R.H. Richter et al., Nucl. Instr. and Meth. A 377 (1996) 412.
[5] I. Abt et al., Double sided microstrip detectors for the high radiation environment in the HERA-B experiment, Talk by S. Masciocchi at the Elmau Conference 1998, Nucl. Instr. and Meth. A 439 (1999) 442.
[6] V.M. Pugatch et al., Radiation hardness of the HERA-B strip detectors, Fourth International Conference on Large Scale Applications and Radiation Hardness of Semiconductor Detectors, June 1999, Florence, Nuovo Cimento, Vol. 112 (2000).
[7] C. Bauer et al., Status of the HERA-B vertex detector, Talk at the VERTEX 99 Conference, Nucl. Instr. and Meth. A, submitted.
[8] F. Klefenz, Die Hochfrequenz-Abschirmung des HERA-B Vertex detektors, Diploma Thesis, Heidelberg, 1997.
[9] W. Fallot-Burghardt et al., HELIX 128-x User Manual, HD-ASIC-33-0697, version 2.1, Heidelberg, 1999.
[10] I. Abt et al., Nucl. Instr. and Meth. A 411 (1999) 191.
[11] I. Abt et al., Nucl. Instr. and Meth. A 423 (1999) 303.
[12] W. Wagner, Auswertung der Daten des HERA-B Vertex detektors im Hinblick auf die physikalischen Eigenschaften der verwendeten Siliziumstreifenzähler, Ph.D. Thesis, München, 2000.
[13] M. Schmelling, The HOLMES program package, HERA-B-99-086.
[14] I. Kisel, S. Masciocchi, CATS: A cellular automaton for tracking in silicon, HERA-B note, in preparation.
[15] I. Kisel et al., Nucl. Instr. and Meth. A 387 (1997) 433.
[16] T. Glebe, I. Kisel, private communication.
[17] M. Dam et al., IEEE Trans. Nucl. Sci. NS-45 (1998) 1787.